

1 **Ocean acidification alters phytoplankton diversity and community structure in the coastal**
2 **water of the East China Sea**

3 Yuming Rao^{#1}, Na Wang^{#2}, He Li³, Jiazhen Sun², Xiaowen Jiang², Di Zhang², Liming Qu², Qianqian
4 Fu², Xuyang Wang², Cong Zhou², Zichao Deng², Yang Tian², Xiangqi Yi², Ruiping Huang², Guang
5 Gao², Xin Lin² and Kunshan Gao^{*1, 3}

6 ¹ State Key Laboratory of Marine Environmental Science, College of the Environment and Ecology,
7 Xiamen University, Xiamen, China

8 ² State Key Laboratory of Marine Environmental Science, College of Ocean and Earth Science,
9 Xiamen University, Xiamen, China

10 ³ Co-Innovation Center of Jiangsu Marine Bio-industry Technology, Jiangsu Ocean University,
11 Lianyungang 222005, China

12 [#] These authors contributed equally to this work

13 ^{*} Correspondence: Kunshao Gao, ksgao@xmu.edu.cn

14 **Keywords:** CO₂, East China Sea, mesocosms; ocean acidification; phytoplankton; primary
15 production

16 **Abstract**

17 Anthropogenic CO₂ emissions and their continuous dissolution into seawater lead to seawater
18 *p*CO₂ rise and ocean acidification (OA). Phytoplankton groups are known to be differentially
19 affected by carbonate chemistry changes associated with OA in different regions of contrasting
20 physical and chemical features. To explore responses of phytoplankton to OA in the Chinese coastal
21 waters, we conducted a mesocosm experiment in a eutrophic bay of the southern East China Sea
22 under ambient (410 μatm, AC) and elevated (1000 μatm, HC) *p*CO₂ levels. The HC condition
23 stimulated phytoplankton growth and primary production during the initial nutrient-replete stage,
24 while the community diversity and evenness in both *p*CO₂ treatments were reduced during this stage
25 due to the rapid nutrient consumption and diatom blooms, and the subsequent shift from diatoms to
26 hetero-dinoflagellates led to a decline in primary production during the mid and later phases under
27 nutrient depletion. HC treatment suppressed the diatom-to-dinoflagellate succession and enhanced
28 the subsequent remineralization of organic matter, thereby facilitating smaller phytoplankton to
29 dominant and sustaining primary production. Our findings indicate that, the impacts of OA on

30 phytoplankton diversity in the coastal water of the southern East China Sea depend on availability
31 of nutrients, with primary productivity and biodiversity of phytoplankton reduced in the
32 eutrophicated coastal water.

33 **1 Introduction**

34 It is commonly known that sequestration of CO₂ in coastal waters play important roles against
35 global warming due to their high primary productivity (Rogelj et al., 2022), which resulted in faster
36 CO₂ removal due to photosynthesis than dissolution of CO₂ from the air (Stukel et al., 2023). It has
37 been assessed that, with the increasing anthropogenic CO₂ emissions, the oceanic CO₂ sink
38 increased from 1.7 ± 0.4 pg C yr⁻¹ in the 1980s to 2.5 ± 0.6 pg C yr⁻¹ in the 2010s (Friedlingstein
39 et al., 2025). Nevertheless, such apparent oceanic CO₂ uptake is altering carbonate chemistry in
40 surface oceans, leading to a pH drop of by 0.017–0.027 units per decade, with a potential further
41 drop by 0.3–0.4 units at the end of this century (Canadell et al., 2023; Gattuso et al., 2015). Such
42 progressive ocean acidification (OA) has been shown to impact many marine organisms (Gattuso et
43 al., 2015), including primary producers (Gao et al., 2020), subsequently feeding back on the CO₂
44 sequestration efficiency in marine systems including coastal waters.

45 OA in eutrophic coastal waters are suggested to progress faster than in open oceans by roughly
46 20 % due to CO₂ dissolution and enhanced remineralization of organic matters (Cai et al., 2011). The
47 subsequent changes in carbonate chemistry may thus drive shifts in phytoplankton community
48 structures/diversity and affect primary productions in differential ways due to regional
49 environmental traits and species-specific physiology (Feng et al., 2024; Gao et al., 2012). While the
50 effects of elevated *p*CO₂ on different phytoplankton assemblages have been demonstrated, positive,
51 neutral and negative effects have been reported, reflecting differences in experimental approaches
52 and/or phytoplankton compositions (Gao et al., 2020). Among the different approaches, field
53 mesocosm experiments under elevated *p*CO₂ projected for future OA scenario have been employed
54 to investigate the effects of OA on ecological processes, including primary production. For example,
55 mesocosm experiments showed that growth of coccolithophores was reduced under 710 μatm *p*CO₂
56 during early summer in 2001 (Engel et al., 2005) and their ability to form blooms disappeared under
57 1000–3000 μatm *p*CO₂ during early summer in 2011 (Riebesell et al., 2017). Under elevated *p*CO₂,
58 phytoplankton communities in Norwegian coastal mesocosms shifted from *Bathycoccus* to

59 *Micromonas* (Meakin and Wyman, 2011). In oligotrophic or mesotrophic conditions, diatoms were
60 insensitive to OA but responded positively under nutrient enrichment (Bach et al., 2019).
61 Furthermore, nutrients enrichment also increased Chl *a* concentration under high $p\text{CO}_2$ condition
62 (Riebesell et al., 2017; Tanaka et al., 2013; Schulz et al., 2013). By contrast, mesocosm experiments
63 conducted in highly eutrophic water showed that high $p\text{CO}_2$ did not affect Chl *a* concentration (Liu
64 et al., 2017). Previously, we showed, by running a mesocosm experiment during spring of 2018 in
65 the southern coastal water of the East China Sea, that elevated $p\text{CO}_2$ of 1000 μatm suppressed the
66 succession from diatoms to dinoflagellates and increased the abundance of viruses and heterotrophic
67 bacteria, promoting refueling of nutrients for phytoplankton growth (Huang et al., 2021). These
68 findings indicate that plankton communities supported by nutrients from remineralization are more
69 sensitive to OA than those having access to higher availability of inorganic nutrients (Bach et al.,
70 2016; Bach et al., 2019). Overall, it is likely that the effects of OA on community structure can vary
71 temporally and spatially, and the availabilities or levels of eutrophication can modulate the effects
72 of OA, alongside regional chemical and physical differences (Paul and Bach, 2020).

73 In coastal regions, changes in seawater carbonate chemistry influence primary production
74 which in reverse affect the pH change due to faster photosynthetic CO_2 removal than its dissolution
75 (Gao, 2021), resulting in increased pH during daytime and declined pH during nighttime. Such large
76 diel pH fluctuation may require phytoplankton to invest more energy to maintain cellular
77 homeostasis in response to the negative effects of increased hydrogen ion concentration (the acidic
78 stress), thereby affecting the functioning of planktonic ecosystem (Raven and Beardall, 2020;
79 Rokitta et al., 2012; Taylor et al., 2017). The positive effects of increased inorganic carbon substrates
80 (e.g., CO_2 and HCO_3^-) and the negative effect of increased H^+ concentration may shape the
81 responses of coastal ecosystems to OA, leading to controversial results (Wu et al., 2017; Vázquez
82 et al., 2023; Chauhan et al., 2024). To better understand the consequences of OA in Chinese
83 eutrophic coastal regions, we conducted a mesocosm experiment in the eutrophic coastal water of
84 Wuyuan Bay, Xiamen, China, using *in situ* plankton communities during October-December, 2019
85 and investigated how OA shapes the diversity of phytoplankton community and affects primary
86 production processes. Our results show that in the eutrophic coastal water of East China Sea, with
87 the natural decrease of temperature, elevated $p\text{CO}_2$ increased primary production by promoting the

88 phytoplankton biomass (indicated by Chl *a* concentration) under nutrient-replete condition, and
89 promoted smaller phytoplankton's growth to sustain the primary production after the nutrient
90 depletion and diatom bloom collapsed, though suppressed the emergence of dinoflagellates.

91 **2 Materials and methods**

92 **2.1 Mesocosms setup and sampling**

93 The *in situ* mesocosm experiment was conducted at the Facility for the Study of Ocean
94 Acidification Impacts of Xiamen University (FOANIC-XMU) located in the subtropical coastal
95 region Wuyuan Bay of southern East China Sea (24.52°N, 117.18°E) from 9th October (day 0
96 relative to algal inoculation) to 14th November, 2019. Nine cylindrical and transparent
97 thermoplastic polyurethane (TPU) mesocosm bags, each 3 m deep and 1.5 m in diameter, were filled
98 with approximately 3000 L of *in situ* seawater that had been prefiltered (MU801-4T, Midea, China,
99 pore size of 0.01 μm). The mesocosms were hooked to and secured within steel frames. Two $p\text{CO}_2$
100 treatments were established to investigate the effects of ocean acidification on the *in situ*
101 phytoplankton community: an ambient $p\text{CO}_2$ treatment (AC, 410 μatm ; 4 numbered bags) and a
102 high $p\text{CO}_2$ treatment representative of end-of-century projections (HC, 1,000 μatm ; 5 numbered
103 bags). To adjust CO_2 in seawater in the HC bags to the projected 1000 μatm in 2100s, approximately
104 11 L of CO_2 -saturated seawater was added to each HC bag. The AC and HC $p\text{CO}_2$ levels were
105 maintained by bubbling with ambient air and pre-mixed air- CO_2 (1000 μatm CO_2), respectively, at
106 a rate of 5 L min^{-1} using a CO_2 Enricher (CE-100B, Wuhan Ruihua Instrument & Equipment Ltd,
107 China). After the carbonate system had been stabilized (leveled pH), 720 L of *in situ* seawater were
108 filtered by a 180 μm mesh to exclude large zooplankton, and each mesocosm bag was inoculated
109 with 80 L of it to initiate the coastal microbial community. Samples were taken from each bag at a
110 depth of 0.5m at 9:00 a.m. by niskin bottles every 1–3 days for physical, chemical and biological
111 analysis.

112 **2.2 Measurement of environmental factors**

113 Solar light intensity was monitored every minute throughout the experimental period using a
114 real-time solar irradiance monitoring device (EKO, Japan). Salinity, temperature and pH in each
115 mesocosm were measured with a salinometer, a digital thermometer and a pH meter (Orino 2 STAR,
116 Thermo Scientific, U. S. A, calibrated with standard NBS buffer), respectively. Dissolved inorganic

117 carbon (DIC) was sampled and measured using an Environmental Water Analyzer (Ma et al., 2018),
118 and total alkalinity (TA) measured using an Automated Spectrophotometric Analyzer (Li et al.,
119 2013). Other seawater carbonate chemistry parameters were calculated with CO2SYS software with
120 known parameters of $p\text{CO}_2$, salinity, pH, temperature, and nutrient concentration.

121 Nutrient samples of each bag were filtered through cellulose acetate membrane (0.22 μm , 47
122 mm), and the filtrate was divided into 2 subsamples; one was stored at $-20\text{ }^\circ\text{C}$ for the measurement
123 of $\text{NO}_3^- + \text{NO}_2^-$, PO_4^{3-} , and NH_4^+ ; another stored at $4\text{ }^\circ\text{C}$ for the measurement of SiO_3^{2-} .
124 Measurement of $\text{NO}_3^- + \text{NO}_2^-$, PO_4^{3-} , and SiO_3^{2-} concentration was conducted using an auto-
125 analyzer (AA3, Seal, Germany), NH_4^+ was measured with indophenol blue spectrophotometry using
126 a spectrophotometer (Tri-223, Spectrum, China) at $25\text{ }^\circ\text{C}$. NO_2^- and NO_3^- were analyzed using the
127 copper-cadmium reduction method, the standard concentrations used for the $\text{NO}_2^- + \text{NO}_3^-$ calibration
128 curve were 0, 1.04, 2.08, 4.16, 10.4, 20.8, and 41.6 μM , and those for NO_2^- calibration curve were
129 0, 0.04, 0.08, 0.16, 0.4, 0.8, and 1.6 μM (Dai et al., 2008). PO_4^{3-} and SiO_3^{2-} were measured using
130 typical spectrophotometric method (Knap et al., 1994), and the calibration curves of both parameters
131 were prepared using standard concentrations of 0, 0.08, 0.16, 0.32, 0.8, 1.6, 3.2 μM and 0, 4, 8, 16,
132 40, 80, 160 μM , respectively.

133 **2.3 Measurement of chlorophyll *a* and particle organic matters**

134 Water samples of each mesocosm (100 – 1000 mL, depending on the biomass in the
135 mesocosms) were filtered onto GF/F filter (Whatman, United States) by suction filter with low
136 vacuum pressure ($<0.02\text{ Mpa}$) and soaked in 5 mL pure methanol overnight. The extracts were
137 centrifuged at $8000 \times g$ and $4\text{ }^\circ\text{C}$ for 10 min, then the absorption spectra of supernatants from 400
138 to 800 nm were measured using a UV-VIS spectrophotometer (DU 800, Beckman, U. S. A). The
139 Chl *a* concentration was calculated according to the following equation (Ritchie, 2006):

$$140 \quad \text{Chl } a \text{ } (\mu\text{g } L^{-1}) = 16.29 \times (A_{665} - A_{750}) - 8.54 \times (A_{652} - A_{750})$$

141 where A_{750} , A_{665} , and A_{652} represents the absorbance of Chl *a* at wave length 750, 665, and
142 652 nm, respectively.

143 For the analysis of particulate organic carbon (POC) and nitrogen (PON) across two particle
144 size fractions, water samples of known volume were first filtered through a 20 μm mesh to obtain
145 subsamples containing particle organic matters smaller than 20 μm . Particles larger than 20 μm

146 (retained on 20 μm mesh) were backwashed using an equal volume of prefiltered (0.22 μm) *in situ*
147 seawater, yielding in subsamples containing particulate organic matters larger than 20 μm . All
148 subsamples were then filtered on pre-combusted (450 $^{\circ}\text{C}$, 6 h) GF/F filter (Whatman) and stored at
149 -20°C until analysis. Before analyses, all filters were fumed over pure HCl for 12 h and dried at
150 60°C to remove inorganic carbon, then packed in tin cups and measured with a CHNS elemental
151 analyzer (Vario EL cube Elementar, Germany).

152 **2.4 Net primary production and dark respiration**

153 Before sunrise, 120 mL of water samples from each mesocosm were collected and dispensed
154 into six 25 mL borosilicate bottles (three bottles for 12 h incubations, and three for 24 h incubations).
155 For each culture duration of each mesocosm, two bottles were illuminated under natural light and
156 one bottle was wrapped tightly in aluminum foil as a dark control. After incubation, cells were
157 filtered onto the GF/F filters (Whatman) under dim light and stored at -20°C . Before measurement,
158 filters were placed individually in 20 mL scintillation vials and exposed to HCl fumes overnight,
159 dried at 60°C for over 6 h to remove any unincorporated $\text{H}^{14}\text{CO}_3^-$. The incorporated ^{14}C by algae
160 was counted with a liquid scintillation counter (Beckman, LS6500, Germany) in the presence of 5
161 mL scintillation cocktail (Hisafe 3, Perkin-Elmer, United States). Nighttime respiratory carbon loss
162 was calculated as the difference between carbon fixation over 12 h (daytime primary production)
163 and 24 h (daily net primary production).

164 **2.5 Determination of phytoplankton biomass and community structure**

165 Water samples (500–2000 mL) from each mesocosm were collected into polyethylene bottles
166 and fixed with 1.5 % acidic lugol's iodine. The samples were statically placed for 2-3 days and
167 concentrated into 50 mL subsamples in the centrifuge tube using siphons within 3 days, then
168 examined with a microscopy (Nikon Eclipse Ns2) and a plankton counting chamber to assess
169 phytoplankton abundance and diversity based on the morphological characteristics as previous
170 described (Hasle and Syvertsen, 1997; Steidinger and Jangen, 1997; Yang and Liu, 2018). To
171 distinguish whether dinoflagellates are autotrophic or heterotrophic, we observed living algal cells
172 in the unstained water samples under the microscope for cell transparency and the presence of
173 chloroplasts.

174 An aliquot of 100 μL for each mesocosm was loaded onto a counting chamber for microscopic

175 enumeration. In each aliquot, the count was deemed valid only when the total number of cells
176 exceeded 200; otherwise, the subsample volume for microscopy was increased to achieve sufficient
177 counts. For samples collected during the exponential growth phase that exhibited excessively high
178 cell densities, appropriate dilution with 0.22 μm -filtered, sterilized seawater was performed prior
179 to counting (State Oceanic Administration 2005).

180 **2.6 Statistical analyses**

181 The data were all expressed by the mean and standard deviation (means \pm SD) and plotted by
182 Origin 2024. Independent-samples *t*-test was conducted to check the significant effects of increased
183 $p\text{CO}_2$ at the level of $p < 0.05$ using SPSS 19. To evaluate α -diversity, Shannon diversity index was
184 calculated based on the relative abundances of phytoplankton taxa using the estimate R and diversity
185 functions from the vegan package (version 2.6-4) in R (Version 4.2.2). Shannon index incorporates
186 both species diversity and evenness. Patterns of physiological parameters over time were
187 emphasizing using generalized additive models (GAMs) and constructed using the 'mgcv' package
188 in R to analyze changes in physiology through the experiment.

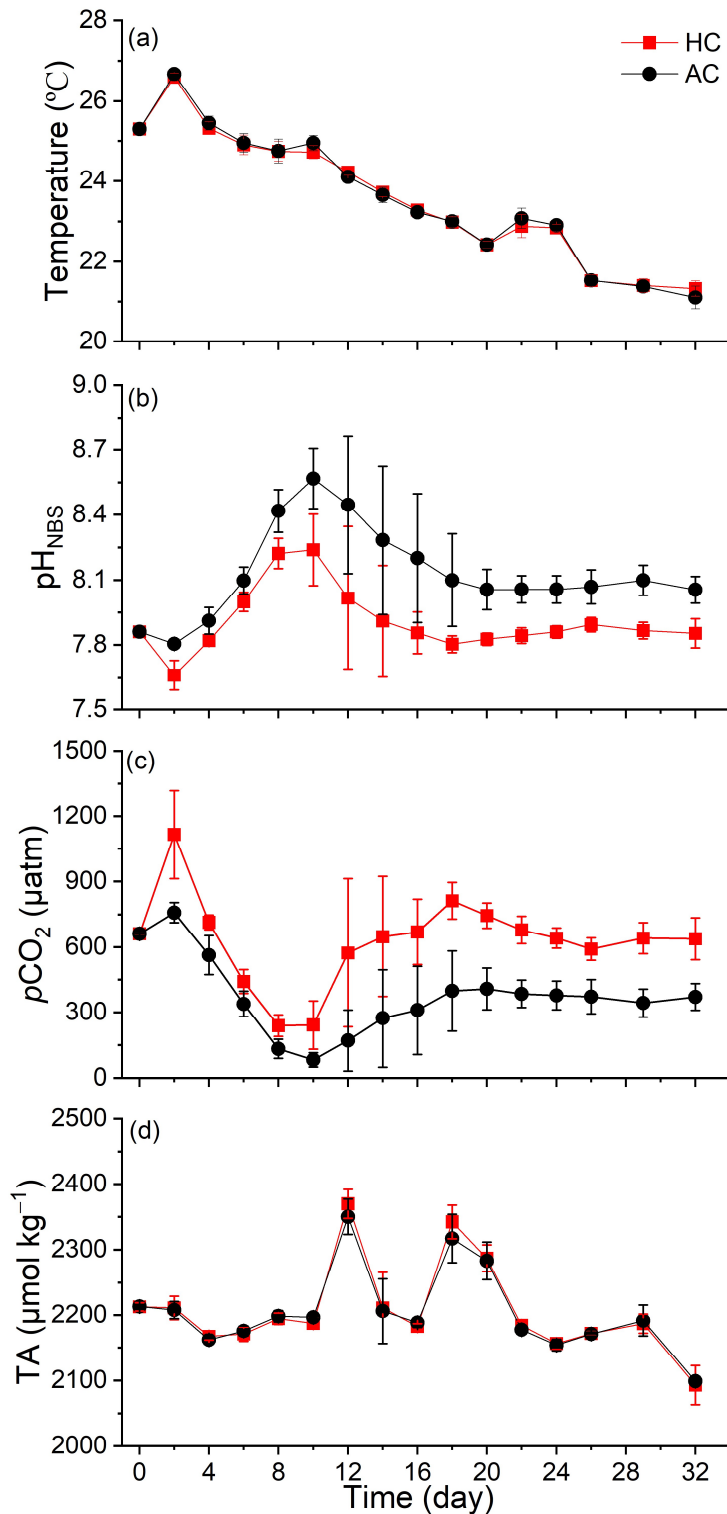
189 **3 Results**

190 **3.1 Environmental changes in the mesocosms**

191 Throughout the experiment, most days were sunny, with daytime mean PAR (12h-average
192 photosynthetic active radiation) ranging from 200 to 850 $\mu\text{mol photons m}^{-2} \text{ s}^{-1}$ (Fig. S1). The
193 environmental temperatures decreased gradually from 26.7 ± 0.05 $^{\circ}\text{C}$ at day 0 (9th October) to 21.1
194 ± 0.28 $^{\circ}\text{C}$ at day 38 (14th November) (Fig. 1 a). Significant differences in pH_{NBS} and $p\text{CO}_2$ between
195 HC and AC were maintained throughout most of the experimental period, while there's no
196 significant difference in total alkalinity (TA) between the two $p\text{CO}_2$ treatments ($p = 4.02 \times 10^{-8}$,
197 2.87×10^{-12} , 0.549, respectively. Figs. 1 b-d, S5 a-c).

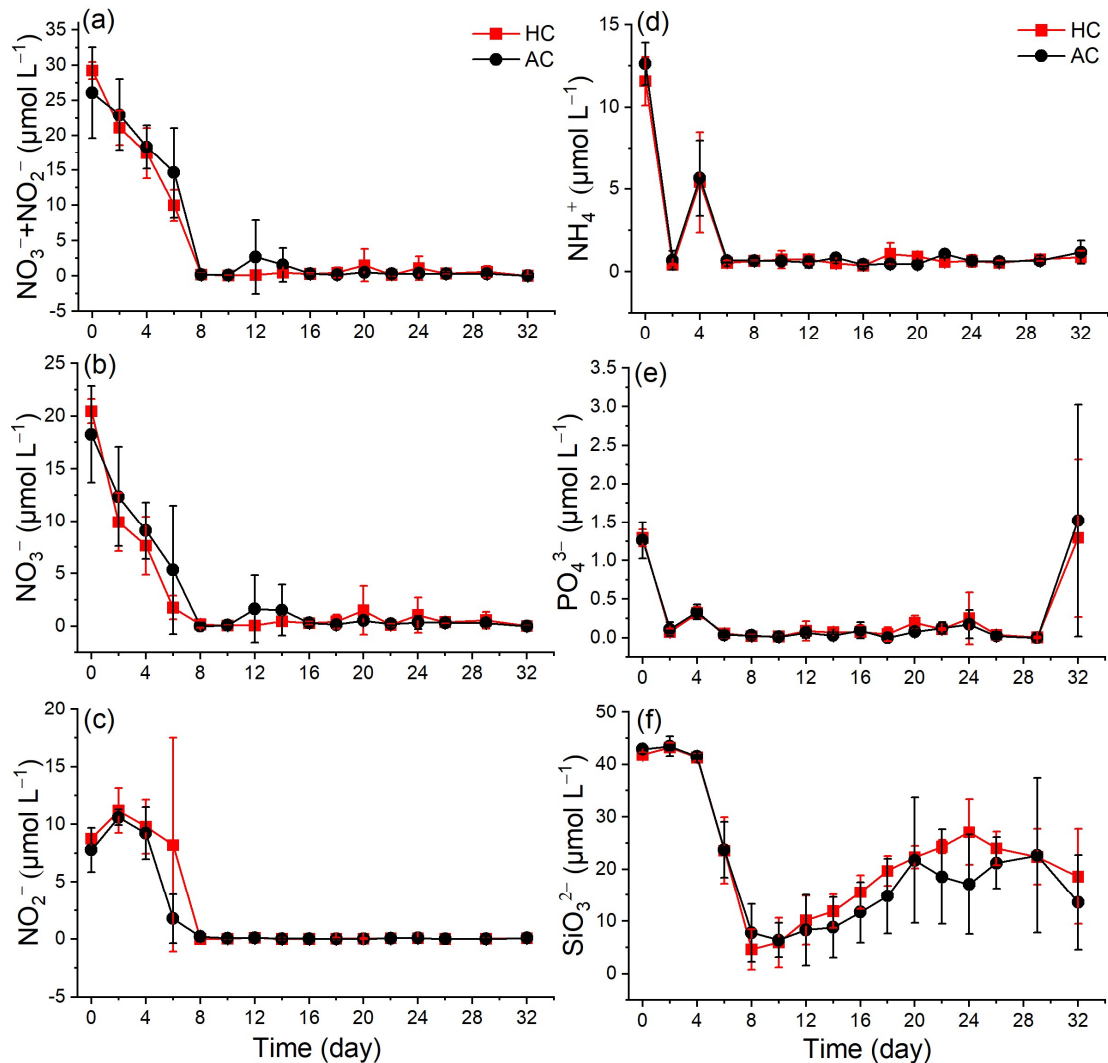
198 Following a sharp increase in phytoplankton biomass from day 4 to day 8 (Fig. 3 a), the pH_{NBS}
199 in the HC and AC mesocosms increased and peaked at 8.24 ± 0.16 and 8.56 ± 0.14 , respectively
200 (Fig. 1 b). Correspondingly, the $p\text{CO}_2$ value dropped to the lowest points of 238.48 ± 49.02 μatm
201 (HC) and 82.82 ± 32.88 μatm (AC) (Fig. 1 c). Then, as the phytoplankton biomass decreased after
202 day 8, pH_{NBS} gradually declined and $p\text{CO}_2$ increased, both stabilizing at relatively constant levels
203 from day 18 until the end of experiment. There were no obvious temporal changes observed in total

204 alkalinity (TA) throughout the experiment (Fig. 1 d).



205

206 Figure 1. Temporal variation of seawater temperature (a), pH_{NBS} (b), pCO₂ (c) and TA (d) in HC
207 (1000 µatm) and AC (410 µatm) mesocosms. The pCO₂ was estimated from the measured pH_{NBS}
208 and DIC concentration using the CO2SYS program. Data are means ± SD of 5 replicates for HC
209 and 4 replicates for AC mesocosms.



211

212 Figure 2. Temporal variation of nutrients (NO_3^- , NO_2^- , $\text{NO}_3^- + \text{NO}_2^-$, NH_4^+ , PO_4^{3-} , and SiO_3^{2-}) in213 HC (1000 μatm) and AC (410 μatm) mesocosms. Data are means \pm SD of 5 replicates for HC and

214 4 replicates for AC mesocosms.

215

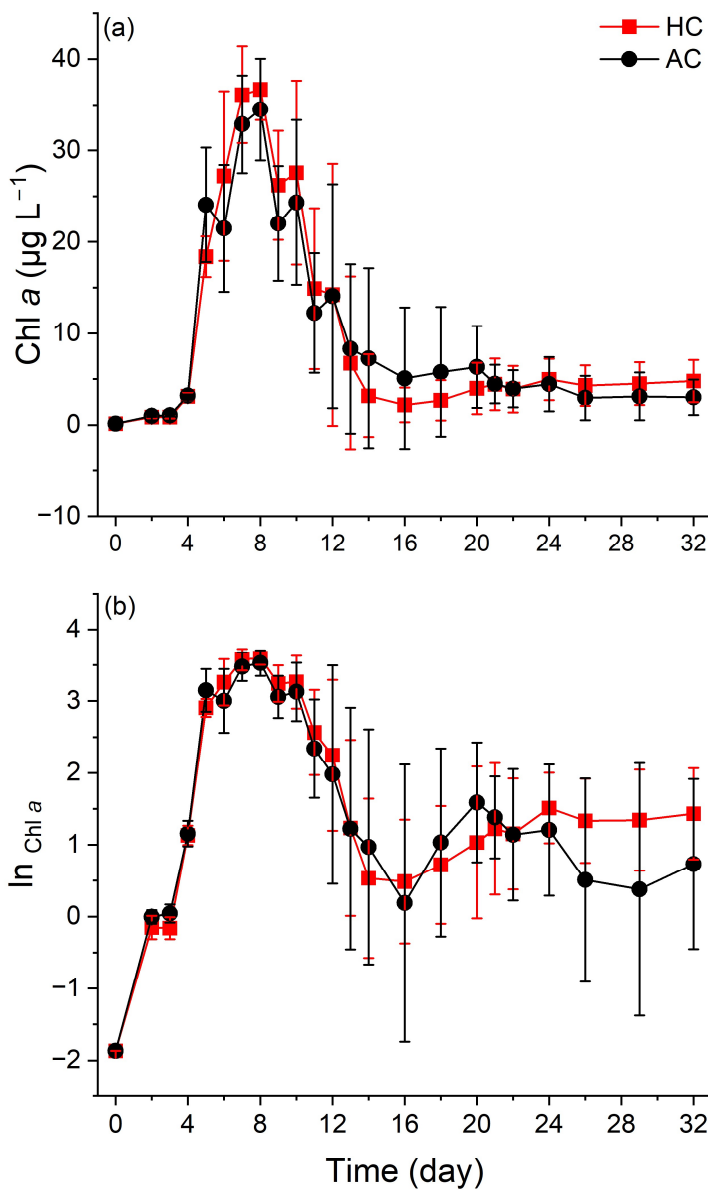
216 The initial nutrient concentrations reflected the eutrophic condition in the coastal seawater

217 ($\text{NO}_3^- + \text{NO}_2^-$: 27 μM , PO_4^{3-} : 1.4 μM). In the mesocosm bags, nutrient concentrations declined218 dramatically in the early phase (up to day 8, Fig. 2). The $\text{NO}_3^- + \text{NO}_2^-$ and NO_3^- concentrations219 decreased sharply to nearly 0 by day 8 (Fig. 2 a, b). In contrast, the NO_2^- concentration experienced

220 a slight increase on day 2, then declined to nearly 0 by day 8 and remained at a low level until the

221 end of experiment in both HC and AC mesocosms (Fig. 2 c). Under HC condition, the NO_3^-

222 concentration decreased more rapidly than that under the AC until day 20, although the difference
 223 was not significant ($p = 0.423$, Fig. S5 d). Both NH_4^+ and PO_4^{3-} concentrations dropped to nearly 0
 224 after 4 days and remain relatively stable thereafter. There were no significant difference observed
 225 between HC and AC mesocosms ($p = 0.579$ and 0.631 , respectively, Figs. 2 d, e, S5 e, f). The SiO_3^{2-}
 226 concentration decreased from $41.81 \pm 0.48 \mu\text{M}$ in HC and $42.88 \pm 0.91 \mu\text{M}$ in AC on day 0 to a
 227 minimum of $4.62 \pm 3.82 \mu\text{M}$ and $7.79 \pm 5.52 \mu\text{M}$ by day 8, respectively. Thereafter, SiO_3^{2-}
 228 concentrations in both HC and AC mesocosms gradually increased until the end of experiment ($p =$
 229 0.343 , Figs. 2 f, S5 g).



230
 231 Figure 3. Temporal variations of Chl *a* concentration (a) and the LN scale of Chl *a* concentration (b)
 232 in HC (1000 μatm) and AC (410 μatm) mesocosms. Data are means \pm SD of 5 replicates for HC and

233 4 replicates for AC mesocosms.

234 **3.2 Chlorophyll *a* concentration**

235 Phytoplankton biomass, indirectly indicated by Chl *a* concentration, increased to peak at 35.88
236 $\pm 3.25 \mu\text{g L}^{-1}$ in the HC and 36.54 ± 4.88 in the AC mesocosms on day 8, and then gradually
237 decreased to $1.12 \pm 0.43 \mu\text{g L}^{-1}$ in HC by day 14 and $0.58 \pm 0.31 \mu\text{g L}^{-1}$ in AC by day 16, followed
238 by a slight increase by the end of experiment (Fig. 3 a). Based on the natural logarithm (ln) scale of
239 Chl *a* concentration, the phytoplankton growth kinetics under the two $p\text{CO}_2$ treatments showed the
240 following phases (Fig. 3 b): the exponential phase (from day 0 to day 5), the stationary phase (from
241 day 6 to day 10), the decline phase (from day 11 to day 16), and a second exponential phase from
242 day 17 to day 24 in the HC and to day 20 in the AC mesocosms. Then, phytoplankton assemblages
243 in the HC mesocosms entered a second stationary phase until the end of experiment, while in the
244 AC ones, they entered a decline phase until day 29, followed by a slight increase on day 32.

245 Throughout the experiment, the elevated $p\text{CO}_2$ resulted in higher average value of Chl *a*
246 concentration at most sampling times, although the differences were not statistically significant (p
247 = 0.142, Fig. S5 h).

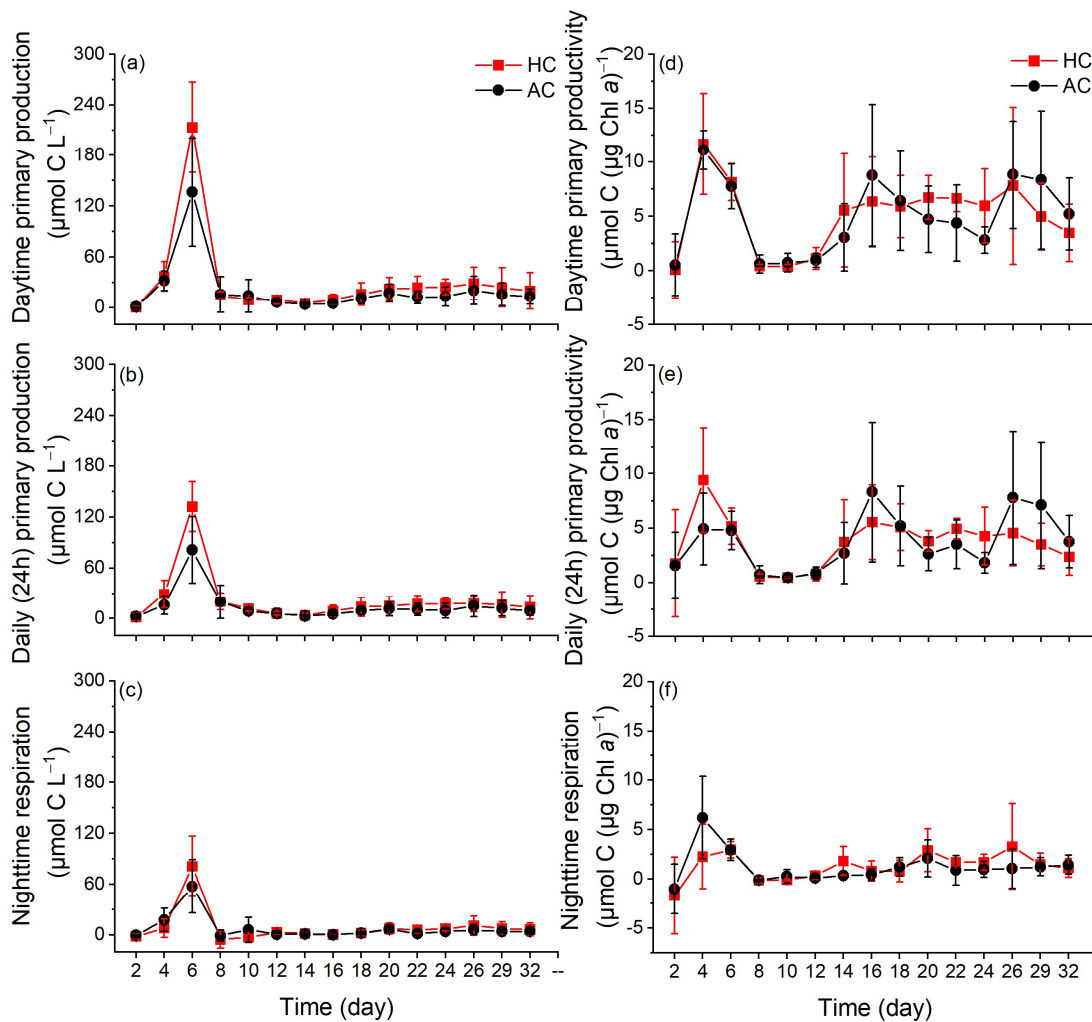
248 **3.3 Primary production and dark respiration**

249 The primary production and night-respiratory per water volume showed patterns similar to
250 those of phytoplankton biomass (indicated by Chl *a* concentration) (Fig. 4, a, b and c). They reached
251 their maximal values on day 6, which corresponded to the end of exponential phase. As the
252 phytoplankton communities entered the stationary phase, daytime (12 h) primary production, daily
253 (24 h) net primary production and nighttime respiration per water volume progressively decreased,
254 and then slightly increased again when the phytoplankton communities underwent the second
255 exponential phase. The elevated $p\text{CO}_2$ increased both daytime and daily net primary production
256 during the middle phase of the experiment, although the positive effect on 24 h primary production
257 tended to decline by the end of experiment ($p = 0.038$ and 0.012 , Fig. S6 a, b). The nighttime
258 respiration of phytoplankton was suppressed before day 8 and enhanced thereafter under the
259 elevated $p\text{CO}_2$, though no significant difference was observed ($p = 0.444$, Fig. S6 c).

260 Primary productivity per Chl *a* increased sharply on day 4, and decreased to the lowest values
261 on day 8. On day 12, both daytime and 24 h primary productivity in the HC increased drastically

262 and then remained relatively stable until the end of experiment (Fig. 4 d, e). In contrast, two
 263 additional peaks were observed in the AC mesocosms on days 16 and 26. The elevated $p\text{CO}_2$
 264 appeared to have enhanced primary productivity from day 2 to day 20, though these effects were
 265 not statistically significant ($p = 0.946$ for daytime and $p = 0.985$ for 24 h, Figs. 4 d, e, S6 d, e).

266 Nighttime respiration per $\mu\text{g Chl } a$ initially increased on day 4, then decreased to nearly zero
 267 in both the HC and AC mesocosms on day 8 and remained relatively stable till the end of experiment.
 268 The elevated $p\text{CO}_2$ had a negative effect on phytoplankton respiration before day 12, but increased
 269 it thereafter, though no significant difference was observed between the HC and AC treatments ($p =$
 270 0.834 , Figs. 4 f, S6 f).



271
 272 Figure 4. The changes of daytime primary production (a) and primary productivity (b), daily (24h)
 273 primary production (c) and primary productivity (d), nighttime respiration per water volume (e) and
 274 per Chl a (f) in HC (1000 μatm) and AC (410 μatm) mesocosms. Data are means \pm SD of 5 replicates

275 for HC and 4 replicates for AC mesocosms.

276

277 **3.4 Changes in Phytoplankton community and diversity**

278 A total of 47 genera identified microscopically include 33 genera of diatoms, 7 of
279 dinoflagellates, 2 of cyanobacteria, 2 of chlorophyta, 2 of cryptophyta and 1 of euglenophyta. In all
280 mesocosms, the dominant species included *Cerataulina pelagica*, *Eucampia cornuta*, *Guinardia*
281 *delicatula*, *Leptocylindrus danicus*, *Skeletonema costatum*, *Protoperidinium* sp., *Gyrodinium*
282 *spirale*, *Cryptophyta* sp. and *Pyramimonas* sp. (Fig. S4).

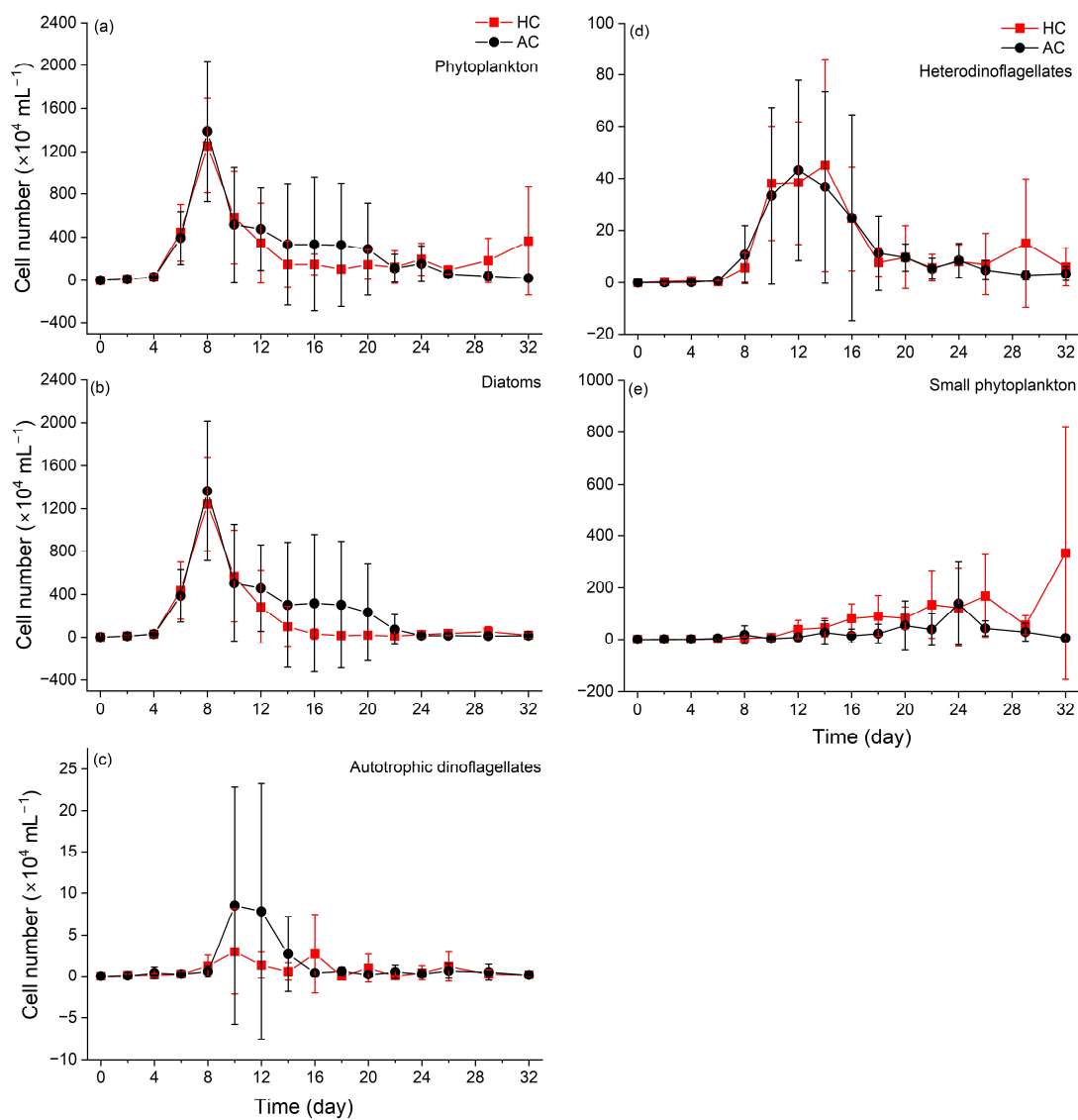
283 Phytoplankton communities underwent dynamic succession in the mesocosms (Fig. 5).
284 Diatoms (mainly *Cerataulina pelagica*) dominated the phytoplankton communities during the early
285 and middle stages of the experiment, as indicated by the similar temporal trends in total
286 phytoplankton and diatom cell counts compared with Chl *a* concentration (Figs. 5 a, b, S4 a). There
287 was no significant difference in diatom density between the HC and AC mesocosms ($p = 0.259$, Fig.
288 S7a), although the average value was lower in the former than in the latter treatment. Autotrophic
289 dinoflagellates began to emerge on day 8 and rapidly declined on day 12 in both HC and AC
290 enclosures (Fig. 5 c). Except for days 6 to 18, the elevated $p\text{CO}_2$ increased the biomass of
291 autotrophic dinoflagellates, though the difference was insignificant ($p = 0.505$, Fig. S7 b). Hetero-
292 dinoflagellates began to emerge on day 6, with their abundance peaked on day 12 in the AC and on
293 day 14 in the HC mesocosms, then decreased by day 22. The elevated $p\text{CO}_2$ did not result in any
294 significant change in terms of their cell numbers ($p = 0.785$, Figs. 5 d, S7 c). On day 26, the biomass
295 of hetero-dinoflagellates increased again in the HC treatment, while it remained constant in the AC
296 treatment ($p = 0.729$, Independent-samples *t*-test).

297 The biomass of small taxa (Cyanobacteria, Chlorophyta, Cryptophyta and Euglenophyta)
298 started to increase on day 8, the HC treatment significantly increased the total biomass of these
299 small phytoplankton species thereafter ($p = 0.019$, Figs. 5 e, S4 h, i, S7 d). From day 22, when
300 diatoms biomass decreased to the lowest level, the temporal variation in small taxa biomass became
301 the main factor controlling overall phytoplankton dynamics (Figs. 5 e, S4 h, i). Accordingly, the
302 positive effect of HC on the small phytoplankton species led to an earlier transition of phytoplankton
303 from the large diatoms and dinoflagellate (mainly fall within the micro size fraction) to the smaller

304 ones (Fig. 6 a, b). This accelerated transition in the HC treatment was also evidenced by higher
 305 concentration of POC and PON in the <20 μm fraction and lower concentration in the >20 μm
 306 fraction (Figs. S2, S3).

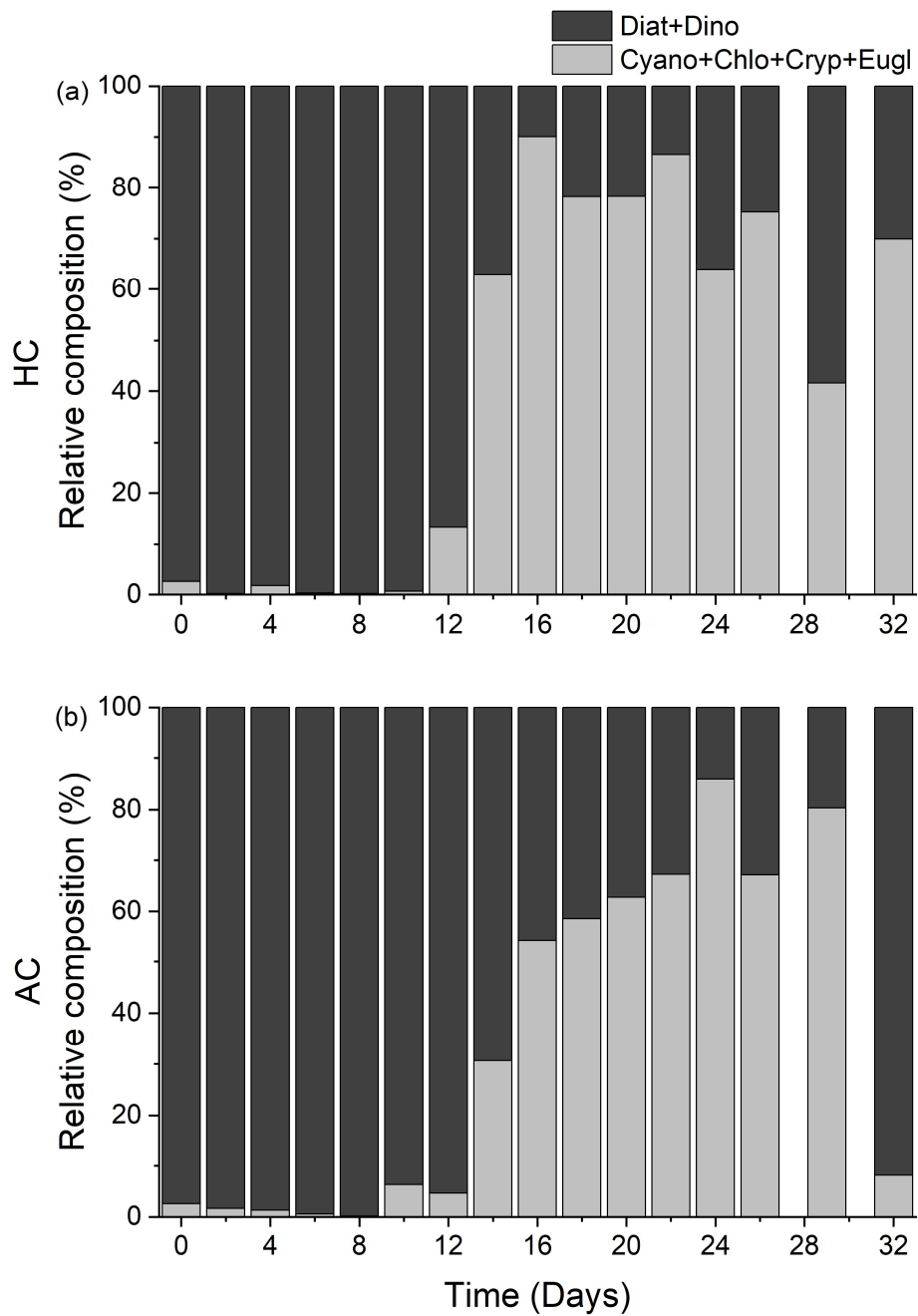
307 In both HC and AC mesocosms, Shannon diversity index decreased sharply from day 2,
 308 reaching the lowest values on day 8 in AC mesocosms and on day 10 in HC mesocosms (Fig. S8 a).
 309 Before day 22, Shannon diversity index increased under elevated $p\text{CO}_2$, whereas it is lowered under
 310 elevated $p\text{CO}_2$ level since day 24, although the differences were not statistically significant ($p =$
 311 0.161, Fig. S8 b).

312



313
 314 Figure 5. Temporal variations of phytoplankton (a), diatoms (b), autotrophic dinoflagellates (c),
 315 heterodinoellagellates (d) and (e) small phytoplankton (Cyanobacteria, Chlorophyta, Cryptophyta

316 and Euglenophyta) cell numbers in HC (1000 μatm) and AC (410 μatm) mesocosms. Data are means
 317 \pm SD of 5 replicates for HC and 4 replicates for AC mesocosms.



318
 319 Figure 6. Temporal variations of the relative composition of diatoms + dinoflagellates (Diat + Dino,
 320 black), Cyanobacteria + Chlorophyta + Cryptophytes + Euglenophyta (Cyano + Chlo + Cryp + Eugl,
 321 grey) in HC (1000 μatm , a) and AC (410 μatm , b) mesocosms. Data are means of 5 replicates for
 322 HC and 4 replicates for AC mesocosms.

323

324 **4 Discussion**

325 Ocean global changes have been suggested to alter community structure and reduce the
326 phytoplankton diversity due to physicochemical environmental changes (Henson et al., 2021; Yuan
327 et al., 2020). Specifically, there appears a growing trend of increasing dinoflagellates abundance
328 relative to diatoms (Carreto et al., 2018). Our mesocosm experiment, conducted in the highly
329 eutrophic Wuyuan Bay in the southern East China Sea during late autumn, also indicated that
330 elevated $p\text{CO}_2$, along with the natural decrease of surface water temperature and declined nutrient
331 availability, altered the structure and diversity of phytoplankton community. The diatom dominance
332 corresponded to the decreased diversity and evenness of phytoplankton community, while these
333 were recovered when the diatom dominance was replaced by dinoflagellates. However, this shift
334 from diatoms to autotrophic dinoflagellates was relatively suppressed under elevated $p\text{CO}_2$
335 conditions. In our mesocosms, the dinoflagellates that emerged during the mid-phase (e.g.,
336 *Protoperidinium* sp., *Pentapharsodinium dalei* and *Heterocapsa* sp., Fig. S9 a) were predominantly
337 small (<20 μm , Fig. S4 g) (Gu et al., 2013; Hanifah et al., 2022), but these dinoflagellates were soon
338 replaced by an even smaller size fraction, including Cyanobacteria, Chlorophyta, Cryptophytes, and
339 Euglenophyta (Figs. 5, 6, S4). Ultimately, these smaller taxa maintained the primary production of
340 phytoplankton communities after nutrient depletion (Fig. 4).

341 When diatoms dominated the phytoplankton community (before day 8), primary production
342 per water volume and per Chl *a* did not change in the same pattern with increased diatom biomass
343 (Fig. 4). This is likely attributable to the larger size of photosynthetic unit (PSU) and lower reaction
344 center-to-Chl *a* ratio in diatoms, which could result in relatively lower photosynthetic efficiency
345 (Wu et al., 2014; Malerba et al., 2018). Meanwhile, The competitive advantages conferred by CO_2 -
346 concentrating mechanisms (CCMs) in diatoms led to insignificant lower biomass (Figs. 5 b, S7 a)
347 but higher primary production per water volume and per μg Chl *a* (Fig. 4 a, b, d and e) under elevated
348 $p\text{CO}_2$: their higher CO_2 affinity and CCMs plasticity may help diatoms gain a competitive advantage
349 in DIC uptake under ocean acidification scenarios (Huang et al., 2021; Raven and Beardall, 2020).
350 Furthermore, the down-regulated of CCMs in diatoms can save energy for other physiology
351 processes and thereby fuel their primary production (see the review by Gao and Campbell, 2014
352 and the references therein). These benefits resulting from elevated $p\text{CO}_2$ also led to higher diversity

353 and evenness (Fig. S8 a, b), suggesting that more diatom species were benefited from the elevated
354 $p\text{CO}_2$. While previous works have demonstrated a positive effect of elevated $p\text{CO}_2$ on the
355 photosynthetic carbon fixation by diatoms grown under low light and phytoplankton assemblages
356 in waters of higher nutrient availability (Gao et al., 2022), our results (Figs. 5 b, S1) indicate that
357 nutrient limitation can override or even reverse to the positive effects of elevated $p\text{CO}_2$ on diatoms
358 (Boyd et al., 2016; Li et al., 2018).

359 It appeared that dinoflagellates were less sensitive to the depletion of nutrients compared to
360 diatoms, with autotrophic dinoflagellates were more sensitive to elevated $p\text{CO}_2$ (Figs. 5 c, S7 b).
361 These suppressed transition from diatoms to autotrophic dinoflagellates under the elevated $p\text{CO}_2$
362 was consistent with our previous works, though conducted in different seasons (Huang et al., 2021),
363 which is likely due to the different CCMs efficiency and/or acidic resilience between dinoflagellates
364 and diatoms. Since the affinity of ribulose 1, 5-diphosphate carboxylase/oxidase (Rubisco) for CO_2
365 is much lower in autotrophic dinoflagellates than in diatoms (Reinfelder, 2011), elevated $p\text{CO}_2$ must
366 have benefitted the former more compared the latter, though invisible growth advantage was
367 observed on the autotrophic dinoflagellates between days 8 and 16. The heterodino­flagellates can
368 utilize organic matters (Glibert and Legrand, 2006) and prey on microbes including bacteria and
369 smaller microalgae (Jeong et al., 2010). This versatile nutrition strategy supported their rapid bloom
370 starting from day 8, leading to the replacement of autotrophic ones from day 12 onward (Fig. 5 c,
371 d). Although they were shown to be insensitive to ocean acidification (Meunier et al., 2017), their
372 respiration was depressed due to the acidic stress, raising their resilience in terms of energetic cost
373 (Wang and Gao, 2024). These mechanisms likely explain the observed insignificant effects of HC
374 on hetero-dinoflagellates.

375 The gradual increase in SiO_3^{2-} concentration, a nutrient exclusively required by diatoms,
376 coincided with their decline, confirming the low abundance of diatoms in the mid and late phase of
377 experiment, while the slightly increases in $\text{NO}_3^- + \text{NO}_2^-$, PO_4^{3-} and SiO_3^{2-} concentrations from day
378 10 onward (Fig. 2 a, e, f) should be attributed to remineralization by heterotrophic bacteria
379 (Aristegui et al., 2009; Bunse and Pinhassi, 2017). These regenerated $\text{NO}_3^- + \text{NO}_2^-$ and PO_4^{3-}
380 subsequently refueled the growth of small phytoplankton taxa, recover the diversity and evenness
381 in the phytoplankton communities (Figs. 5 e, S8 a, b) (Thingstad and Rassoulzadegan, 1995).

382 Alternatively, it is plausible that grazing activity by zooplankton, which was not quantified in this
383 study, also contributed to the apparent rise in diversity and evenness, as grazers tend to consume
384 dominant phytoplankton taxa (Thingstad and Rassoulzadegan, 1999; Calbet and Landry, 2004).

385 The dominant small taxa, such as *Cryptophyta* sp. and green microalga *Pyramimonas* sp. (Fig.
386 S4 h, i) during days 16–24, achieved primary productivity (per $\mu\text{g Chl } a$) comparable to the diatom-
387 dominated community observed on days 4–6 (Fig. 4 b, d). The success of these small taxa after
388 nutrient depletion can be attributed to their small size and larger surface-to-volume ratio (Finkel et
389 al., 2009; Giordano et al., 2005), which might enable them with higher efficiency in nutrients uptake
390 and CO_2 diffusion. Furthermore, the higher abundance of viruses and heterotrophic bacteria in the
391 HC mesocosms (Huang et al., 2021; Lin et al., 2018) intensified nutrient remineralization,
392 subsidizing these small, fast-growing phototrophs and leading to their earlier emergence on day 16
393 compared to day 24 in the AC mesocosms (Fig. 6). While it's possible that picophytoplankton
394 originally present in this region (Zhong et al., 2020) were missed by microscope-based identification,
395 it is reasonable to infer that they also contributed to the late-phase primary production. Previous
396 studies indicated that, after diatom/dinoflagella blooms and nutrient depletion, remineralized
397 nutrients in the seawater may also favor the growth of picophytoplankton (Nishibe et al., 2015; Fu
398 et al., 2009) and elevated $p\text{CO}_2$ would further benefit their growth. Thus, it is likely that,
399 picophytoplankton also dominated the phytoplankton communities in the HC mesocosms.

400 Though previous studies have suggested the changing temperatures influenced the
401 phytoplankton growth and community structure individually or interactively with OA and other
402 environmental factors (Bénard et al., 2018; Courboulès et al., 2018; Li et al., 2018), the results from
403 the present autumn mesocosm experiment revealed the same pattern with our previous spring
404 mesocosm experiment (Huang et al., 2021), suggesting that it is not the seasonal temperature
405 trajectories but the availability of nutrients that controlled the shift from diatom to dinoflagellate
406 dominance, leading to declines in primary productivity (Huang et al., 2021; Cloern, 1996). Such
407 consistency underscores that nutrient availability and stoichiometry are the primary determinants of
408 phytoplankton community composition, usually exerting stronger and more immediate effects on
409 taxonomic and functional group dominance (Karl et al., 1996; Paerl and Paul, 2012; Ptacnik et al.,
410 2008; Meyer et al., 2016), though thermal and acidic stresses can impact phytoplankton

411 photosynthesis and respiration to greater extent under nutrient limitation (Li et al., 2018; Gao et al.,
412 2022).

413 Reduced nutrient availability usually decreases phytoplankton community richness (Gazeau et
414 al., 2017), although ocean acidification appeared to partly offset such effects (Fig. S8). However,
415 these compensatory effects diminished once both the initial and regenerated nitrogen sources were
416 exhausted (after day 24, Fig. S8 b). At that point, only a few small phytoplankton taxa tolerant to
417 low pH remained dominant, indicating a loss of diversity in the community and less stable
418 ecosystems (McCann, 2000) under combination of acidic stress and nutrient limitation. In summary,
419 beyond compensating previous works, our study further demonstrated that progressive ocean
420 acidification is likely to reduce primary production and phytoplankton diversity in the eutrophicated
421 coastal water of the southern East China Sea.

422 **Data availability Statement**

423 All relevant data are presented in the paper and its Supporting Information file, and will be available
424 upon request to the corresponding author Kunshan Gao.

425 **Conflict of Interest**

426 The authors declare no competing interests.

427 **Acknowledgements**

428 This study was supported by the National Key Research and Development Program of China
429 (2022YFC3105303), the National Natural Science Foundation of China (42361144840,
430 41720104005). We are grateful to the engineers, Xianglan Zeng and Wenyan Zhao, for their
431 technical supports, and we thank Prof. Jian Ma (College of the Environment and Ecology, Xiamen
432 University) for providing the Environmental Water Analyzer (iSEA) during the mesocosm
433 experiment.

434 **Author's Contributions**

435 Kunshan Gao and Guang Gao designed the mesocosm experiment; Yuming Rao, Na Wang, Jiazhen
436 Sun, Xiaowen Jiang, Di Zhang, Liming Qu, He Li, Qianqian Fu, Xuyang Wang, Cong Zhou, Zichao
437 Deng, Yang Tian, Xiangqi Yi, Ruiping Huang performed the mesocosm experiment; Yuming Rao
438 analyzed the data and wrote up the manuscript; Na Wang performed microscopy observation;
439 Kunshan Gao edited the manuscript; All authors reviewed and contributed to revision of the

440 manuscript.

441

442 **References**

443 Arístegui, J., Gasol, J. M., Duarte, C. M., and Herndl, G. J.: Microbial oceanography of the dark ocean's
444 pelagic realm, *Limnol. Oceanogr.*, 54, 1501-1529, <https://doi.org/10.4319/lo.2009.54.5.1501>, 2009.

445 Bach, L. T., Hernández-Hernández, N., Taucher, J., Spisla, C., Sforza, C., Riebesell, U., and Arístegui,
446 J.: Effects of Elevated CO₂ on a Natural Diatom Community in the Subtropical NE Atlantic, *Front.*
447 *Mar. Sci.*, Volume 6 - 2019, 10.3389/fmars.2019.00075, 2019.

448 Bach, L. T., Taucher, J., Boxhammer, T., Ludwig, A., The Kristineberg, K. C., Achterberg, E. P., Algueró-
449 Muñiz, M., Anderson, L. G., Bellworthy, J., Büdenbender, J., Czerny, J., Ericson, Y., Esposito, M.,
450 Fischer, M., Haunost, M., Hellemann, D., Horn, H. G., Hornick, T., Meyer, J., Sswat, M., Zark, M.,
451 and Riebesell, U.: Influence of Ocean Acidification on a Natural Winter-to-Summer Plankton
452 Succession: First Insights from a Long-Term Mesocosm Study Draw Attention to Periods of Low
453 Nutrient Concentrations, *Plos One*, 11, e0159068, 10.1371/journal.pone.0159068, 2016.

454 Bénard, R., Levasseur, M., Scarratt, M., Blais, M. A., Mucci, A., Ferreyra, G., Starr, M., Gosselin, M.,
455 Tremblay, J. É., and Lizotte, M.: Experimental assessment of the sensitivity of an estuarine
456 phytoplankton fall bloom to acidification and warming, *Biogeosciences*, 15, 4883-4904,
457 10.5194/bg-15-4883-2018, 2018.

458 Boyd, P. W., Dillingham, P. W., McGraw, C. M., Armstrong, E. A., Cornwall, C. E., Feng, Y. y., Hurd, C.
459 L., Gault-Ringold, M., Roleda, M. Y., Timmins-Schiffman, E., and Nunn, B. L.: Physiological
460 responses of a Southern Ocean diatom to complex future ocean conditions, *Nat. Clim. Change.*, 6,
461 207-213, 10.1038/nclimate2811, 2016.

462 Bunse, C. and Pinhassi, J.: Marine Bacterioplankton Seasonal Succession Dynamics, *Trends. Microbiol.*,
463 25, 494-505, <https://doi.org/10.1016/j.tim.2016.12.013>, 2017.

464 Cai, W.-J., Hu, X., Huang, W.-J., Murrell, M. C., Lehrter, J. C., Lohrenz, S. E., Chou, W.-C., Zhai, W.,
465 Hollibaugh, J. T., and Wang, Y.: Acidification of subsurface coastal waters enhanced by
466 eutrophication, *Nat. Geosci.*, 4, 766-770, 2011.

467 Calbet, A. and Landry, M. R.: Phytoplankton growth, microzooplankton grazing, and carbon cycling in
468 marine systems, *Limnol. Oceanogr.*, 49, 51-57, <https://doi.org/10.4319/lo.2004.49.1.0051>, 2004.

469 Canadell, J. G., Monteiro, P. M., Costa, M. H., Cotrim da Cunha, L., Cox, P. M., Eliseev, A. V., Henson,
470 S., Ishii, M., Jaccard, S., and Koven, C.: Intergovernmental Panel on Climate Change (IPCC).
471 Global carbon and other biogeochemical cycles and feedbacks, in: Climate change 2021: The
472 physical science basis. Contribution of working group I to the sixth assessment report of the
473 intergovernmental panel on climate change, Cambridge University Press, 673-816, 2023.

474 Carreto, J. I., Carignan, M. O., Montoya, N. G., Cozzolino, E., and Akselman, R.: Mycosporine-like
475 amino acids and xanthophyll-cycle pigments favour a massive spring bloom development of the
476 dinoflagellate *Prorocentrum minimum* in Grande Bay (Argentina), an ozone hole affected area, *J.*
477 *Marine. Syst.*, 178, 15-28, <https://doi.org/10.1016/j.jmarsys.2017.10.004>, 2018.

478 Chauhan, N., Dedman, C. J., Baldreki, C., Dowle, A. A., Larson, T. R., and Rickaby, R. E. M.: Contrasting
479 species-specific stress response to environmental pH determines the fate of coccolithophores in
480 future oceans, *Mar. Pollut. Bull.*, 209, 117136, <https://doi.org/10.1016/j.marpolbul.2024.117136>,
481 2024.

482 Cloern, J. E.: Phytoplankton bloom dynamics in coastal ecosystems: A review with some general lessons
483 from sustained investigation of San Francisco Bay, California, *Rev. Geophys.*, 34, 127-168,
484 <https://doi.org/10.1029/96RG00986>, 1996.

485 Courboulès, J., Vidussi, F., Soulié, T., Mas, S., Pecqueur, D., and Mostajir, B.: Effects of experimental
486 warming on small phytoplankton, bacteria and viruses in autumn in the Mediterranean coastal Thau
487 Lagoon, *Aquatic Ecology*, 55, 647-666, [10.1007/s10452-021-09852-7](https://doi.org/10.1007/s10452-021-09852-7), 2021.

488 Dai, M., Wang, L., Guo, X., Zhai, W., Li, Q., He, B., and Kao, S. J.: Nitrification and inorganic nitrogen
489 distribution in a large perturbed river/estuarine system: the Pearl River Estuary, China,
490 *Biogeosciences*, 5, 1227-1244, [10.5194/bg-5-1227-2008](https://doi.org/10.5194/bg-5-1227-2008), 2008.

491 Engel, A., Zondervan, I., Aerts, K., Beaufort, L., Benthien, A., Chou, L., Delille, B., Gattuso, J.-P., Harlay,
492 J., and Heemann, C.: Testing the direct effect of CO₂ concentration on a bloom of the
493 coccolithophorid *Emiliana huxleyi* in mesocosm experiments, *Limnol. Oceanogr.*, 50, 493-507,
494 2005.

495 Feng, Y., Xiong, Y., Hall-Spencer, J. M., Liu, K., Beardall, J., Gao, K., Ge, J., Xu, J., and Gao, G.: Shift
496 in algal blooms from micro- to macroalgae around China with increasing eutrophication and climate
497 change, *Global Change Biol.*, 30, e17018, <https://doi.org/10.1111/gcb.17018>, 2024.

498 Finkel, Z. V., Beardall, J., Flynn, K. J., Quigg, A., Rees, T. A. V., and Raven, J. A.: Phytoplankton in a
499 changing world: cell size and elemental stoichiometry, *J. Plankton. Res.*, 32, 119-137,
500 10.1093/plankt/fbp098, 2009.

501 Friedlingstein, P., O'Sullivan, M., Jones, M. W., Andrew, R. M., Hauck, J., Landschützer, P., Le Quéré,
502 C., Li, H., Luijkx, I. T., Olsen, A., Peters, G. P., Peters, W., Pongratz, J., Schwingshackl, C., Sitch,
503 S., Canadell, J. G., Ciais, P., Jackson, R. B., Alin, S. R., Arneeth, A., Arora, V., Bates, N. R., Becker,
504 M., Bellouin, N., Berghoff, C. F., Bittig, H. C., Bopp, L., Cadule, P., Campbell, K., Chamberlain,
505 M. A., Chandra, N., Chevallier, F., Chini, L. P., Colligan, T., Decayeux, J., Djéutchouang, L. M.,
506 Dou, X., Duran Rojas, C., Enyo, K., Evans, W., Fay, A. R., Feely, R. A., Ford, D. J., Foster, A.,
507 Gasser, T., Gehlen, M., Gkritzalis, T., Grassi, G., Gregor, L., Gruber, N., Gürses, Ö., Harris, I.,
508 Hefner, M., Heinke, J., Hurtt, G. C., Iida, Y., Ilyina, T., Jacobson, A. R., Jain, A. K., Jarníková, T.,
509 Jersild, A., Jiang, F., Jin, Z., Kato, E., Keeling, R. F., Klein Goldewijk, K., Knauer, J., Korsbakken,
510 J. I., Lan, X., Lauvset, S. K., Lefèvre, N., Liu, Z., Liu, J., Ma, L., Maksyutov, S., Marland, G., Mayot,
511 N., McGuire, P. C., Metzl, N., Monacci, N. M., Morgan, E. J., Nakaoka, S. I., Neill, C., Niwa, Y.,
512 Nützel, T., Olivier, L., Ono, T., Palmer, P. I., Pierrot, D., Qin, Z., Resplandy, L., Roobaert, A., Rosan,
513 T. M., Rödenbeck, C., Schwinger, J., Smallman, T. L., Smith, S. M., Sospedra-Alfonso, R., Steinhoff,
514 T., Sun, Q., Sutton, A. J., Séférian, R., Takao, S., Tatebe, H., Tian, H., Tilbrook, B., Torres, O.,
515 Tourigny, E., Tsujino, H., Tubiello, F., van der Werf, G., Wanninkhof, R., Wang, X., Yang, D., Yang,
516 X., Yu, Z., Yuan, W., Yue, X., Zaehle, S., Zeng, N., and Zeng, J.: Global Carbon Budget 2024, *Earth*
517 *Syst. Sci. Data*, 17, 965-1039, 10.5194/essd-17-965-2025, 2025.

518 Fu, M., Wang, Z., Li, Y., Li, R., Sun, P., Wei, X., Lin, X., and Guo, J.: Phytoplankton biomass size
519 structure and its regulation in the Southern Yellow Sea (China): Seasonal variability, *Cont. Shelf*
520 *Res.*, 29, 2178-2194, <https://doi.org/10.1016/j.csr.2009.08.010>, 2009.

521 Gao, K.: Approaches and involved principles to control pH/pCO₂ stability in algal cultures, *J. Appl.*
522 *Phycol*, 33, 3497-3505, 2021.

523 Gao, K. and Campbell, D. A.: Photophysiological responses of marine diatoms to elevated CO₂ and
524 decreased pH: a review, *Funct. Plant. Biol.*, 41, 449-459, <https://doi.org/10.1071/FP13247>, 2014.

525 Gao, K., Zhao, W., and Beardall, J.: Future responses of marine primary producers to environmental
526 changes, *Blue Planet, Red and Green Photosynthesis: Productivity and Carbon Cycling in Aquatic*

527 Ecosystems, 273-304, 2022.

528 Gao, K., Gao, G., Wang, Y., and Dupont, S.: Impacts of ocean acidification under multiple stressors on
529 typical organisms and ecological processes, *Mar. Life. Sci. Tech.*, 2, 279-291, 2020.

530 Gao, K., Xu, J., Gao, G., Li, Y., Hutchins, D. A., Huang, B., Wang, L., Zheng, Y., Jin, P., and Cai, X.:
531 Rising CO₂ and increased light exposure synergistically reduce marine primary productivity, *Nat.*
532 *Clim. Change.*, 2, 519-523, 2012.

533 Gattuso, J.-P., Magnan, A., Billé, R., Cheung, W. W., Howes, E. L., Joos, F., Allemand, D., Bopp, L.,
534 Cooley, S. R., and Eakin, C. M.: Contrasting futures for ocean and society from different
535 anthropogenic CO₂ emissions scenarios, *Science*, 349, aac4722, 2015.

536 Gazeau, F., Sallon, A., Pitta, P., Tsiola, A., Maugendre, L., Giani, M., Celussi, M., Pedrotti, M. L., Marro,
537 S., and Guieu, C.: Limited impact of ocean acidification on phytoplankton community structure and
538 carbon export in an oligotrophic environment: Results from two short-term mesocosm studies in the
539 Mediterranean Sea, *Estuar. Coast. Shelf. S.*, 186, 72-88, <https://doi.org/10.1016/j.ecss.2016.11.016>,
540 2017.

541 Giordano, M., Norici, A., and Hell, R.: Sulfur and phytoplankton: acquisition, metabolism and impact on
542 the environment, *New. Phytol.*, 166, 371-382, 2005.

543 Glibert, P. M. and Legrand, C.: The Diverse Nutrient Strategies of Harmful Algae: Focus on Osmotrophy,
544 in: *Ecology of Harmful Algae*, edited by: Granéli, E., and Turner, J. T., Springer Berlin Heidelberg,
545 Berlin, Heidelberg, 163-175, 10.1007/978-3-540-32210-8_13, 2006.

546 Gu, H., Luo, Z., Zeng, N., Lan, B., and Lan, D.: First record of *Pentapharsodinium* (Peridinales,
547 Dinophyceae) in the China Sea, with description of *Pentapharsodinium dalei* var. *aciculiferum*,
548 *Phycological Research*, 61, 256-267, <https://doi.org/10.1111/pre.12024>, 2013.

549 Hanifah, A. H., Teng, S. T., Law, I. K., Abdullah, N., Chiba, S. U. A., Lum, W. M., Tillmann, U., Lim, P.
550 T., and Leaw, C. P.: Six marine thecate *Heterocapsa* (Dinophyceae) from Malaysia, including the
551 description of three novel species and their cytotoxicity potential, *Harmful. algae.*, 120, 102338,
552 <https://doi.org/10.1016/j.hal.2022.102338>, 2022.

553 Hasle, G. R. and Syvertsen, E. E.: Chapter 2 - Marine Diatoms, in: *Identifying Marine Phytoplankton*,
554 edited by: Tomas, C. R., Academic Press, San Diego, 5-385, [https://doi.org/10.1016/B978-](https://doi.org/10.1016/B978-012693018-4/50004-5)
555 [012693018-4/50004-5](https://doi.org/10.1016/B978-012693018-4/50004-5), 1997.

556 Henson, S. A., Cael, B. B., Allen, S. R., and Dutkiewicz, S.: Future phytoplankton diversity in a changing
557 climate, *Nat. Commun.*, 12, 5372, 10.1038/s41467-021-25699-w, 2021.

558 Huang, R., Sun, J., Yang, Y., Jiang, X., Wang, Z., Song, X., Wang, T., Zhang, D., Li, H., and Yi, X.:
559 Elevated $p\text{CO}_2$ Impedes Succession of Phytoplankton Community From Diatoms to Dinoflagellates
560 Along With Increased Abundance of Viruses and Bacteria, *Front. Mar. Sci.*, 8, 642208, 2021.

561 Jeong, H. J., Yoo, Y. D., Kim, J. S., Seong, K. A., Kang, N. S., and Kim, T. H.: Growth, feeding and
562 ecological roles of the mixotrophic and heterotrophic dinoflagellates in marine planktonic food
563 webs, *Ocean. Sci. J.*, 45, 65-91, 10.1007/s12601-010-0007-2, 2010.

564 Karl, D. M., Christian, J. R., Dore, J. E., Hebel, D. V., Letelier, R. M., Tupas, L. M., and Winn, C. D.:
565 Seasonal and interannual variability in primary production and particle flux at Station ALOHA,
566 *Deep-Sea. Res. Pt. II*, 43, 539-568, [https://doi.org/10.1016/0967-0645\(96\)00002-1](https://doi.org/10.1016/0967-0645(96)00002-1), 1996.

567 Knap, A., Michaels, A., Close, A., Ducklow, H., and Dickson, A.: Protocols for the Joint Global Ocean
568 Flux Study (JGOFS) core measurements, vi+170 pp.1994.

569 Li, F., Beardall, J., and Gao, K.: Diatom performance in a future ocean: interactions between nitrogen
570 limitation, temperature, and CO_2 -induced seawater acidification, *ICES. J. Mar. Sci.*, 75, 1451-1464,
571 10.1093/icesjms/fsx239, 2018.

572 Li, Q., Wang, F., Wang, Z. A., Yuan, D., Dai, M., Chen, J., Dai, J., and Hoering, K. A.: Automated
573 Spectrophotometric Analyzer for Rapid Single-Point Titration of Seawater Total Alkalinity, *Environ.*
574 *Sci. Technol.*, 47, 11139-11146, 10.1021/es402421a, 2013.

575 Lin, X., Huang, R., Li, Y., Li, F., Wu, Y., Hutchins, D. A., Dai, M., and Gao, K.: Interactive network
576 configuration maintains bacterioplankton community structure under elevated CO_2 in a eutrophic
577 coastal mesocosm experiment, *Biogeosciences*, 15, 551-565, 10.5194/bg-15-551-2018, 2018.

578 Liu, N., Tong, S., Yi, X., Li, Y., Li, Z., Miao, H., Wang, T., Li, F., Yan, D., Huang, R., Wu, Y., Hutchins,
579 D. A., Beardall, J., Dai, M., and Gao, K.: Carbon assimilation and losses during an ocean
580 acidification mesocosm experiment, with special reference to algal blooms, *Mar. Environ. Res.*, 129,
581 229-235, <https://doi.org/10.1016/j.marenvres.2017.05.003>, 2017.

582 Ma, J., Li, P., Chen, Z., Lin, K., Chen, N., Jiang, Y., Chen, J., Huang, B., and Yuan, D.: Development of
583 an Integrated Syringe-Pump-Based Environmental-Water Analyzer (iSEA) and Application of It for
584 Fully Automated Real-Time Determination of Ammonium in Fresh Water, *Anal. Chem.*, 90, 6431-

585 6435, 10.1021/acs.analchem.8b01490, 2018.

586 McCann, K. S.: The diversity–stability debate, *Nature*, 405, 228-233, 10.1038/35012234, 2000.

587 Meakin, N. G. and Wyman, M.: Rapid shifts in picoeukaryote community structure in response to ocean
588 acidification, *ISME J.*, 5, 1397-1405, 10.1038/ismej.2011.18, 2011.

589 Meunier, C. L., Algueró-Muñiz, M., Horn, H. G., Lange, J. A. F., and Boersma, M.: Direct and indirect
590 effects of near-future CO₂ levels on zooplankton dynamics, *Mar. Freshwater Res.*, 68, 373-380,
591 <https://doi.org/10.1071/MF15296>, 2017.

592 Meyer, J., Löscher, C. R., Neulinger, S. C., Reichel, A. F., Loginova, A., Borchard, C., Schmitz, R. A.,
593 Hauss, H., Kiko, R., and Riebesell, U.: Changing nutrient stoichiometry affects phytoplankton
594 production, DOP accumulation and dinitrogen fixation – a mesocosm experiment in the eastern
595 tropical North Atlantic, *Biogeosciences*, 13, 781-794, 10.5194/bg-13-781-2016, 2016.

596 Nishibe, Y., Takahashi, K., Shiozaki, T., Kakehi, S., Saito, H., and Furuya, K.: Size-fractionated primary
597 production in the Kuroshio Extension and adjacent regions in spring, *J. Oceanogr.*, 71, 27-40,
598 10.1007/s10872-014-0258-0, 2015.

599 Paerl, H. W. and Paul, V. J.: Climate change: Links to global expansion of harmful cyanobacteria, *Water*
600 *Res.*, 46, 1349-1363, <https://doi.org/10.1016/j.watres.2011.08.002>, 2012.

601 Paul, A. J. and Bach, L. T.: Universal response pattern of phytoplankton growth rates to increasing CO₂,
602 *New Phytol.*, 228, 1710-1716, <https://doi.org/10.1111/nph.16806>, 2020.

603 Ptacnik, R., Solimini, A. G., Andersen, T., Tamminen, T., Brettum, P., Lepistö, L., Willén, E., and
604 Rekolainen, S.: Diversity predicts stability and resource use efficiency in natural phytoplankton
605 communities, *Proc. Natl. Acad. Sci.*, 105, 5134-5138, doi:10.1073/pnas.0708328105, 2008.

606 Raven, J. A. and Beardall, J.: Energizing the plasmalemma of marine photosynthetic organisms: the role
607 of primary active transport, *J. Mar. Biol. Assoc. Uk.*, 100, 333-346, 2020.

608 Reinfelder, J. R.: Carbon concentrating mechanisms in eukaryotic marine phytoplankton, *Annu. Rev.*
609 *Mar. Sci.*, 3, 291-315, 2011.

610 Riebesell, U., Bach, L. T., Bellerby, R. G., Monsalve, J. R. B., Boxhammer, T., Czerny, J., Larsen, A.,
611 Ludwig, A., and Schulz, K. G.: Competitive fitness of a predominant pelagic calcifier impaired by
612 ocean acidification, *Nat. Geosci.*, 10, 19-23, 2017.

613 Ritchie, R. J.: Consistent sets of spectrophotometric chlorophyll equations for acetone, methanol and

614 ethanol solvents, *Photosynth. Res.*, 89, 27-41, 2006.

615 Rogelj, J., Shindell, D., Jiang, K., Fifita, S., Forster, P., Ginzburg, V., Handa, C., Kheshgi, H., Kobayashi,
616 S., Kriegler, E., Mundaca, and L., S., R., and Vilariño, M. V: Mitigation Pathways Compatible with
617 1.5°C in the Context of Sustainable Development, in: *Global Warming of 1.5°C: IPCC Special*
618 *Report on Impacts of Global Warming of 1.5°C above Pre-industrial Levels in Context of*
619 *Strengthening Response to Climate Change, Sustainable Development, and Efforts to Eradicate*
620 *Poverty*, edited by: Intergovernmental Panel on Climate, C., Cambridge University Press,
621 Cambridge, 93-174, DOI: 10.1017/9781009157940.004, 2022.

622 Rokitta, S. D., John, U., and Rost, B.: Ocean acidification affects redox-balance and ion-homeostasis in
623 the life-cycle stages of *Emiliana huxleyi*, *Plos One*, 7, e52212, 2012.

624 Schulz, K. G., Bellerby, R. G. J., Brussaard, C. P. D., Büdenbender, J., Czerny, J., Engel, A., Fischer, M.,
625 Koch-Klavnsen, S., Krug, S. A., Lischka, S., Ludwig, A., Meyerhöfer, M., Nondal, G., Silyakova, A.,
626 Stuhr, A., and Riebesell, U.: Temporal biomass dynamics of an Arctic plankton bloom in response
627 to increasing levels of atmospheric carbon dioxide, *Biogeosciences*, 10, 161-180, 10.5194/bg-10-
628 161-2013, 2013.

629 Steidinger, K. A. and Jangen, K.: Chapter 3 - Dinoflagellates, in: *Identifying Marine Phytoplankton*,
630 edited by: Tomas, C. R., Academic Press, San Diego, 387-584, [https://doi.org/10.1016/B978-](https://doi.org/10.1016/B978-012693018-4/50005-7)
631 [012693018-4/50005-7](https://doi.org/10.1016/B978-012693018-4/50005-7), 1997.

632 Stukel, M. R., Irving, J. P., Kelly, T. B., Ohman, M. D., Fender, C. K., and Yingling, N.: Carbon
633 sequestration by multiple biological pump pathways in a coastal upwelling biome, *Nat. Commun.*,
634 14, 2024, 10.1038/s41467-023-37771-8, 2023.

635 Tanaka, T., Alliouane, S., Bellerby, R. G. B., Czerny, J., de Kluijver, A., Riebesell, U., Schulz, K. G.,
636 Silyakova, A., and Gattuso, J. P.: Effect of increased $p\text{CO}_2$ on the planktonic metabolic balance
637 during a mesocosm experiment in an Arctic fjord, *Biogeosciences*, 10, 315-325, 10.5194/bg-10-
638 315-2013, 2013.

639 Taylor, A. R., Brownlee, C., and Wheeler, G.: Coccolithophore cell biology: chalking up progress, *Annu.*
640 *Rev. Mar. Sci.*, 9, 283-310, 2017.

641 Thingstad, T. F. and Rassoulzadegan, F.: Nutrient limitations, microbial food webs and 'biological C-
642 pumps': suggested interactions in a P-limited Mediterranean, *Mar. Ecol. Prog. Ser.*, 117, 299-306,

643 1995.

644 Thingstad, T. F. and Rassoulzadegan, F.: Conceptual models for the biogeochemical role of the photic
645 zone microbial food web, with particular reference to the Mediterranean Sea, *Prog. Oceanogr.*, 44,
646 271-286, [https://doi.org/10.1016/S0079-6611\(99\)00029-4](https://doi.org/10.1016/S0079-6611(99)00029-4), 1999.

647 Vázquez, V., León, P., Gordillo, F. J. L., Jiménez, C., Concepción, I., Mackenzie, K., Bresnan, E., and
648 Segovia, M.: High-CO₂ Levels Rather than Acidification Restrict *Emiliana huxleyi* Growth and
649 Performance, *Microb. Ecol.*, 86, 127-143, [10.1007/s00248-022-02035-3](https://doi.org/10.1007/s00248-022-02035-3), 2023.

650 Wang, N. and Gao, K.: Ocean acidification and food availability impacts on the metabolism and grazing
651 in a cosmopolitan herbivorous protist *Oxyrrhis marina*, *Front. Mar. Sci.*, Volume 11 - 2024,
652 [10.3389/fmars.2024.1371296](https://doi.org/10.3389/fmars.2024.1371296), 2024.

653 Wu, Y., Campbell, D. A., and Gao, K.: Short-term elevated CO₂ exposure stimulated photochemical
654 performance of a coastal marine diatom, *Mar. Environ. Res.*, 125, 42-48,
655 <https://doi.org/10.1016/j.marenvres.2016.12.001>, 2017.

656 Yang, S. and Liu, X.: Characteristics of phytoplankton assemblages in the southern Yellow Sea, China,
657 *Mar. Pollut. Bull.*, 135, 562-568, 2018.

658 Yuan, Z., Liu, D., Masqué, P., Zhao, M., Song, X., and Keesing, J. K.: Phytoplankton Responses to
659 Climate-Induced Warming and Interdecadal Oscillation in North-Western Australia, *Paleoceanogr.*
660 *Paleocl.*, 35, e2019PA003712, <https://doi.org/10.1029/2019PA003712>, 2020.

661 Zhong, Y., Liu, X., Xiao, W., Laws, E. A., Chen, J., Wang, L., Liu, S., Zhang, F., and Huang, B.:
662 Phytoplankton community patterns in the Taiwan Strait match the characteristics of their realized
663 niches, *Prog. Oceanogr.*, 186, 102366, 2020.